1970

A technique for cooling single crystals below 90°K for x-ray diffraction, and the crystal structures of H2Ta6Cl18.6H2O, and the photodimer of 1, 1-dimethyl-2, 5-diphenyl-l-silacyclopentadiene

Charles Burton Thaxton
Iowa State University

71-7334

THAXTON, Charles Burton, 1939-

A TECHNIQUE FOR COOLING SINGLE CRYSTALS BELOW 90°K FOR X-RAY DIFFRACTION, AND THE CRYSTAL STRUCTURES OF $H_2Ta_6Cl_{18} \cdot 6H_2O$, AND THE PHOTODIMER OF 1,1-DIMETHYL-2,5-DIPHENYL-1-SILACYCLOPENTADIENE.

Iowa State University, Ph.D., 1970
Chemistry, physical
University Microfilms, Inc., Ann Arbor, Michigan

A TECHNIQUE FOR COOLING SINGLE CRYSTALS BELOW 90°K FOR X-RAY DIFFRACTION, AND THE CRYSTAL STRUCTURES OF $H_2Ta_6Cl_{18}\cdot 6H_2O$, AND THE PHOTODIMER OF 1,1-DIMETHYL-2,5-DIPHENYL-1-SILACYCLOPENTADIENE

by

Charles Burton Thaxton

A Dissertation Submitted to the
Graduate Faculty in Partial Fulfillment of
The Requirements for the Degree of
DOCTOR OF PHILOSOPHY

Major Subject: Physical Chemistry

Approved:

Signature was redacted for privacy.

In Charge of Major Work

Signature was redacted for privacy.

Head of Major Department

Signature was redacted for privacy.

Dean of Graduate College

Iowa State University
Of Science and Technology
Ames, Iowa

1970

TABLE OF CONTENTS

DEDICATION

T L

INTRODUCTION

The X-ray crystallographic method has been used in recent years to determine more molecular structures than all other experimental methods combined. The application of this important method of structural analysis can be summarized in seven parts.

(1) Select and mount single crystal of appropriate dimensions. It is not uncommon that difficulty in acquiring suitable single crystals constitutes the chief hindrance to structural analysis.

(2) Preliminary X-ray photographs. These photographs are used to obtain approximate unit cell dimensions and to establish the space group (if unique), or at least limit the choice of possible space groups.

(3) Data collection (raw intensities). Although film methods are still quite common, the counter diffractometer method of data collection is becoming increasingly employed since it offers the possibility for more accurate intensities (perhaps 3 to 4 times) and is also readily adapted to automated use. Whereas one may estimate ~500 intensities per day using film methods (which is a full-time operation), it is not uncommon to collect ~1000 intensities per day with an automated counter diffractometer which requires only a minimum of operator attention. This ease of data collection has prompted many non-crystallographers to incorporate the X-ray method of structure determination into their research programs.

(4) Data reduction (corrected intensities). This step includes at least correction for Lorentz-polarization effects. The Lorentz correction arises because of geometrical effects, i.e., the crystal motion produced by the instrument used in the data collection. The polarization

correction is necessary due to the partially polarized nature of the reflected X-ray beam, and is therefore a function only of 2θ, the scattering angle. Other effects which may need to be taken into account are those due to absorption, extinction, streak, and anomalous dispersion.

(5) Solution of phase problem and the derived structure. Although a number of techniques are available for arrival at an appropriate trial model (Patterson, superposition, direct methods, etc.) none is guaranteed for a given problem. Therefore this step in the analysis may not proceed routinely.

The general expression in trigonometric form relating corrected intensities to structure factors is

$$I_{hkl}^{cor.} = F_{hkl}^2 = \left(\sum_{j=1}^{m} f_j \text{ Cos } 2\pi(hx_j + ky_j + lz_j)\right)^2 + \left(\sum_{j=1}^{m} f_j \text{ Sin } 2\pi(hx_j + ky_j + lz_j)\right)^2 \quad (1)$$

In this expression f_j is the atomic scattering factor for atom j; x_j, y_j, and z_j are the fractional coordinates for atom j in the unit cell, while h, k, and l are the crystallographic indices for the reflection. This expression can be simplified considerably for the special case involving a center of symmetry, which is the case for the two structures presented in this thesis. Since a center of symmetry transforms (x,y,z) into $(\bar{x},\bar{y},\bar{z})$, expression (1) immediately reduces to (2) if the origin is placed at a center of symmetry.

$$I_{hkl}^{cor} = F_{hkl}^2 = \left(\sum_{j=1}^{m} f_j \text{ Cos } 2\pi(hx_j + ky_j + lz_j)\right)^2 \quad (2)$$

Since one does not usually know the coordinates to be used in expression (2), another function, called the electron density function, has been devised and is usually employed in crystal structure analysis. The electron density function, a Fourier series describing the density of scattering matter within the unit cell, is given in expression (3) for the special case involving a center of symmetry.

$$\rho(xyz) = \frac{1}{V} \sum_{-\infty}^{\infty} \sum_{-\infty}^{\infty} \sum_{-\infty}^{\infty} F_{hkl} \cos 2\pi \left(\frac{hx}{a} + \frac{ky}{b} + \frac{lz}{c} \right) \qquad (3)$$

Only the unit cell dimensions and magnitudes of F_{hkl} are known from experiment. In practice one arrives at an appropriate trial model (any method that works) whose coordinates "fix" the phase or sign of F_{hkl} for each reflection, thus giving the electron density at each particular set of coordinates. Successive structure factor and electron density map calculations are especially helpful in suggesting changes in the trial model.

(6) Refinement of derived structure. In recent years the method of least-squares has been the usual approach in refinement of the derived structure. Formerly this important step was often the most laborious in structure analysis. However, since the advent of high speed computers the refinement step is perhaps the most routine, if not straight-forward, of all the steps. One generally refines scale factors, as well as fractional coordinates and thermal parameters (isotropic and/or anisotropic) for the individual atoms, ions or molecules in the asymetric unit of the structure.

(7) Presentation of results. The final step in an analysis of a crystal structure is the presentation of results. This presentation usually includes observed and calculated structure factors, bond distances

and angles with associated standard deviations, intermolecular distances, stereographic drawings showing the unit cell and individual views of ions or molecules, and results of thermal motion analysis. These and other details one may wish to include depending on the particular problem involved.

Let us assume an experimental arrangement for collecting intensities such that a counter diffractometer is employed at room temperature. Further let us suppose that sufficient data are collected such that the estimated standard deviation in the bond length is ± 0.005 Å. If a 0.1% significance level is considered valid, then a difference between two bond lengths of greater than 0.015 Å may be taken as significant. However, it is not uncommon in crystals, especially organic ones, that thermal motion causes an apparent atomic displacement of 0.02 Å or more. Since it is generally recognized that corrections for thermal motion are somewhat approximate, it would be beneficial if thermal motion could be minimized.

The scattering factor falls off with increasing $\text{Sin } \theta/\lambda$ (which falloff is due to the finite size of the electron cloud about the nucleus) as shown by

$$f = f_o e^{-B \text{ Sin}^2 \theta/\lambda^2} \qquad (4)$$

where f and f_o are the scattering factors at angles θ and 0^o, respectively. In this expression B is a function related to the root-mean-square amplitude of vibration, often called the temperature factor which is somewhat of a misnomer. In many crystals thermal motion, indicated by the value of B, can be reduced to a third its room temperature value by cooling to 90^oK. In addition to reducing systematic errors in the coordinates, low

temperatures allow one to collect more data, further improving statistics.

Although molecular parameters via the X-ray method generally have been less accurate than those obtained by spectroscopic methods, the former should become more competitive by utilizing both counter diffractometer data and low temperature ($\sim 90^{\circ}K$). This thesis describes the analysis of two crystal structures and presents an experimental technique for cooling single crystals during data collection to temperatures below $90^{\circ}K$.

PART I. CRYSTAL STRUCTURE OF 1,1-DIMETHYL-2, 5-DIPHENYL-1-SILACYCLOPENTADIENE PHOTODIMER

Introduction

Schmidt, et al. (1-10) have advanced the thesis, called the topochemical postulate, that "reaction in the solid state occurs with a minimun amount of atomic or molecular movement." It has been further suggested that for nearest neighbor reactive center ($\geq C=C \leq$) separations of greater than about 4.1 Å, solid state photo-dimerization is prevented.

Barton (11) has successfully photo-dimerized 1,1-dimethyl-2,5-diphenyl-1-silacyclopentadiene (silole monomer) in the solid state, and Clardy and Read (12) have recently determined the single crystal X-ray structure of this monomer. Shortest separation of nearest neighbor reactive centers ($\geq C=C \leq$) in this monomer crystal are significantly longer (~6.5 Å) than the apparent 4.1 Å photo active upper limit suggested by Schmidt (3) and indicates marked departure from his data. Lattice geometry of the monomer seemed to favor the centric dimer, and "spectral data does not necessitate a 'head-to-tail' dimer nor does it specify the stereochemistry of the cyclobutane ring" (13). Therefore, we felt a single crystal X-ray study of silole dimer to firmly establish the path of this photo-dimerization would be of interest.

Experimental

Single crystals of the compound were kindly supplied by Barton. Microscopic examination revealed that the crystals were elongated parallelepipeds with well-defined edges. Since there was no evidence of decomposition in the atmosphere, a single crystal was selected and mounted

on the end of a glass fiber with Duco cement. Precession photographs exhibited only $\bar{1}$ symmetry indicating a triclinic space group. Intensity statistics (14) indicated the centrosymmetric space group $P\bar{1}$, as was later confirmed by successful refinement of the derived structure.

Crystal data

1,1-dimethyl-2,5-diphenyl-1-silacyclopentadiene photo-dimer (silole dimer); $Si_2C_{36}H_{36}$; M = 524.85; M.P. 197-8°C; triclinic, space group $P\bar{1}(C_i^1)$; lattice parameters at 23±3°C for the crystal used in the data collection, $\underline{a}$ = 13.137 ± 5, $\underline{b}$ = 11.601 ± 3, $\underline{c}$ = 11.252 ± 4 Å, α = 95.94 ± 2°, β = 77.91 ± 3°, γ = 116.51 ± 2°, V = 1500.39 Å^3. The reduced cell in conventional orientation (15) is: $\underline{a}$ = 11.601 ± 3, $\underline{b}$ = 13.081 ± 5, $\underline{c}$ = 11.252 ± 4 Å, α = 96.81 ± 3°, β = 95.94 ± 2°, γ = 116.01 ± 2°, V = 1500.39 Å^3; d_{obsd} = 1.1 ± 1 g/cm^3(by flotation), d_{calcd} = 1.051 g/cm^3 for Z = 2 formula units of $Si_2C_{36}H_{36}$ per unit cell; F(000) = 560; μ = 11.8 cm^{-1} for Cu-Kα radiation; color: colorless; crystal habit: parallelepiped, elongated along $\underline{c}$ direction of non-reduced cell.

The lattice parameters and their standard deviations were obtained by a least-squares (16) fit to 27 independent reflection angles with theta above 20°.

Data collection and treatment of data

For data collection, a crystal having approximate dimensions 0.25 x 0.20 x 0.30 mm was mounted such that the 0.2 mm axis was along the spindle axis. Data were collected at 23 ± 3°C utilizing a four-circle Hilger-Watts automated diffractometer interfaced to an SDS 910 computer. Using nickel filtered copper Kα radiation (λ = 1.542 Å) all data in the four octants with

positive l-index were recorded within a theta sphere of 55^{o} using the stationary-crystal, stationary-counter technique. Counting times were 5 and 10 sec for the background and peak, respectively. As a check on electronic and crystal stability, three standard reflections (600, 004, and 240) were remeasured periodically during the data collection period. These exhibited some unusual fluctuations which prompted us to remeasure all reflections. The same crystal orientation was used in both data collections.

The measured intensities were corrected for background, and for Lorentz-polarization effects. No correction for absorption was made since the maximum and minimum transmission factors were 0.77 and 0.68 (17), respectively (μ = 11.8 cm^{-1}). Of the 8133 independent pieces of data (including duplicate and some multiple observations), 2215 were found to have values of measured intensity, I_o, less than three times the standard error based on counting statistics. These reflections were considered as unobserved and were not included in the solution and refinement of the structure.

The estimated error in each intensity measurement was calculated by

$$[\sigma(I_o)]^2 = [C_t + C_b + (K_t * C_t)^2 + (K_b * C_b)^2] / (Lp)^2$$

where C_t and C_b are the total count and the background count, respectively, while Lp is the Lorentz-polarization correction. A value of 0.05 was arbitrarily assigned to K_t and K_b, the fractional random errors in C_t and C_b. The estimated standard deviation in each structure factor was calculated by

$$\sigma(F_o) = [(I_o) + \sigma(I_o)]^{1/2} - |F_o|$$

a function based on the finite difference method (18).

Since sporadic difficulties had been encountered in the diffractometer system, a unique set of data was obtained by devising a model independent statistical test for the F_o's, observed structure factors. When F_o's from both data sets agreed within five standard deviations they were averaged, as were the standard deviations of the F_o's; otherwise they were removed from further consideration. Utilization of this statistical test with subsequent averaging yielded a total of 2154 unique pieces of observed data, as compared to a total of 2658 pieces of data prior to the test. Although this is quite a stringent device it does appear to be justifiable owing to the random nature of the errors involved. The arithmetic mean was applied to the F_o's while standard deviations in F_o were calculated by

$$[\sigma(F_o)]_{avg.} = \{\Sigma[\sigma(F_o)]^2\}^{1/2}/N$$

where N is the total number of terms in the summation. These standard deviations were used during the least-squares refinements to weight the observed structure factor, where w, the individual weighting factor was defined as $1/[\sigma(F_o)]^2$.

Solution of Structure

Examination of the sharpened (19) Patterson function revealed the positions of the silicon atoms. Successive structure factor and electron density map (20) calculations readily revealed the remaining non-hydrogen atom locations. These positions were then refined by full-matrix least-squares (21) techniques with isotropic thermal parameters to a conventional discrepancy index of $R = \Sigma \, ||F_o| - |F_c||/\Sigma|F_o| = 21.6\%$ and a weighted

R-factor of $\omega R = (\Sigma\omega(|F_o| - |F_c|)^2 / \Sigma\omega|F_o|^2)^{1/2} = 28.8\%$. Cromer and Waber (22) scattering factors were used with no correction for anomalous dispersion effects. A difference electron density map at this stage indicated that all non-hydrogen atoms had been accounted for, but that considerable anisotropic motion was present. Although a significant number of the observed reflections were eliminated from the refinement as previously described, sufficient data were still available to justify carrying out full-matrix anisotropic least-squares refinement on all non-hydrogen atoms (~7 reflections per variable).

Prior to anisotropic refinement, 20 reflections were noted with $|F_o - F_c| > 20\sigma(F_o)$ and were discarded. Final anisotropic values of R and ωR of 9.0% and 12.3%, respectively, were obtained. A final electron density difference map was calculated showing no peak greater than a few tenths of 1 electron/$\AA^3$, except in suspected hydrogen atom locations.

Final values of the positional parameters for silole dimers A and B together with the standard deviations as derived from the inverse matrix of the last cycle of the least-squares refinement are given in Tables 1 and 2, respectively. An indication of the directions and root-mean square amplitudes of vibration for the atoms refined anisotropically is provided by Tables 3 and 4 for dimers A and B, respectively. In Figure 1 are given the values of F_o and F_c in electrons (x100) for the 2134 reflections used in the final refinement. A structure factor calculation was also carried out with the original set of 2658 reflections and gave a conventional R-index of 14.5%. In addition, the values of F_c for reflections considered unobserved were computed and in no case exceeded $3\sigma(F_o)$.

Table 1. Final values of the positional parameters and their standard deviations for silole dimer A

Atom	X/a	Y/b	Z/c
Si (A)	0.1696(1)	-0.0681(1)	0.0300(1)
C(1A)	0.1130(6)	-0.1171(6)	0.1949(5)
C(2A)	0.3195(5)	0.0012(7)	-0.0092(6)
C(3A)	0.0969(5)	0.0421(5)	-0.0059(4)
C(4A)	0.0096(4)	-0.0424(5)	-0.0914(4)
C(5A)	0.0201(5)	-0.1659(5)	-0.1279(4)
C(6A)	0.0887(4)	-0.1952(4)	-0.0809(4)
C(7A)	0.1915(5)	0.1677(5)	-0.0515(4)
C(8A)	0.2379(5)	0.1914(6)	-0.1744(5)
C(9A)	0.3304(7)	0.3040(7)	-0.4162(6)
C(10A)	0.3885(6)	0.3971(7)	-0.1383(6)
C(11A)	0.3452(6)	0.3774(6)	-0.0178(8)
C(12A)	0.2472(5)	0.2634(6)	0.0318(6)
C(13A)	0.1064(5)	-0.3127(5)	-0.1161(5)
C(14A)	0.0883(5)	-0.3720(6)	-0.2328(6)
C(15A)	0.1062(6)	-0.4815(7)	-0.2637(7)
C(16A)	0.1450(6)	-0.5329(6)	-0.1822(8)
C(17A)	0.1637(7)	-0.4723(7)	-0.0666(7)
C(18A)	0.1462(6)	-0.3637(6)	-0.0366(6)

[a]Numbers in parenthesis represent standard deviations in the last digit of the parameter.

Table 2. Final values of the positional parameters and their standard deviations for silole dimer B

Atom	X/a	Y/b	Z/c
Si(B)	0.5173(1)	0.2133(1)	0.4156(1)
C(1B)	0.5562(6)	0.1962(6)	0.2438(5)
C(2B)	0.5878(6)	0.3885(5)	0.4580(6)
C(3B)	0.5460(5)	0.1058(5)	0.5089(5)
C(4B)	0.4261(4)	0.0062(4)	0.5691(4)
C(5B)	0.3313(5)	0.0346(5)	0.5436(5)
C(6B)	0.3592(5)	0.1373(5)	0.4728(5)
C(7B)	0.6310(5)	0.1917(5)	0.5921(5)
C(8B)	0.5863(6)	0.2159(5)	0.7122(5)
C(9B)	0.6657(8)	0.3022(7)	0.7831(6)
C(10B)	0.7805(8)	0.3640(7)	0.7333(8)
C(11B)	0.8266(6)	0.3431(6)	0.6138(6)
C(12B)	0.7483(6)	0.2530(6)	0.5470(5)
C(13B)	0.2760(5)	0.1820(5)	0.4521(5)
C(14B)	0.1625(7)	0.1314(8)	0.5147(6)
C(15B)	0.0131(7)	0.1873(10)	0.4997(7)
C(16B)	0.1262(9)	0.2883(9)	0.4259(7)
C(17B)	0.2350(8)	0.3375(7)	0.3616(7)
C(18B)	0.3120(6)	0.2832(6)	0.3740(6)

[a]Numbers in parentheses represent standard deviations in the last digit of the parameter.

Table 3. Final values of the thermal parameters and their standard deviations for silole dimer A. The form of the temperature factor is $\exp(-\beta_{11}h^2 - \beta_{22}k^2 - \beta_{33}\ell^2 - 2\beta_{12}hk - 2\beta_{13}h\ell - 2\beta_{23}k\ell)$

Atom	β_{11}	β_{22}	β_{33}	β_{12}	β_{13}	β_{23}
Si(A)	144(2)	144(2)	135(1)	85(1)	-59(1)	-21(1)
C(1A)	218(8)	217(8)	137(5)	127(7)	-66(6)	- 7(5)
C(2A)	129(6)	217(8)	248(9)	87(6)	-67(6)	-31(6)
C(3A)	127(5)	152(6)	115(4)	71(5)	-46(4)	-19(4)
C(4A)	141(6)	142(5)	137(5)	77(5)	-66(5)	-32(4)
C(5A)	140(6)	166(6)	136(5)	86(5)	-51(5)	-19(4)
C(6A)	119(5)	135(5)	136(5)	63(4)	-26(4)	- 5(4)
C(7A)	140(6)	139(6)	140(5)	82(5)	-41(5)	-17(4)
C(8A)	144(7)	162(7)	162(6)	74(6)	-31(5)	7(5)
C(9A)	175(8)	198(9)	213(8)	81(7)	-48(7)	8(7)
C(10A)	184(9)	220(9)	173(7)	94(7)	-37(7)	8(6)
C(11A)	139(7)	160(8)	317(12)	65(C)	-88(8)	-40(7)
C(12A)	154(7)	142(7)	212(7)	68(6)	-79(6)	-32(5)
C(13A)	134(6)	145(6)	163(6)	74(5)	-41(5)	-18(4)
C(14A)	157(7)	179(7)	192(7)	91(6)	-62(6)	-62(6)
C(15A)	174(8)	184(8)	282(11)	91(7)	-74(8)	-95(8)
C(16A	162(8)	160(7)	316(12)	83(6)	-52(8)	-19(8)
C(17A)	221(10)	197(9)	268(10)	130(8)	-70(8)	-11(7)
C(18A)	186(8)	212(8)	177(7)	127(7)	-32(6)	6(6)

Table 4. Final values of the thermal parameters and their standard deviations for silole dimer B. The form of the temperature factor is $\exp(-\beta_{11}h^2 - \beta_{22}k^2 - \beta_{33}\ell^2 - 2\beta_{12}hk - 2\beta_{13}h\ell - 2\beta_{23}k\ell)$

Atom	β_{11}	β_{22}	β_{33}	β_{12}	β_{13}	β_{23}
Si(B)	146(2)	137(2)	141(2)	69(1)	- 52(1)	- 9(1)
C(1B)	200(9)	233(9)	153(6)	118(7)	- 37(6)	8(5)
C(2B)	196(8)	138(6)	241(8)	80(6)	- 99(7)	-17(5)
C(3B)	145(6)	125(5)	164(5)	68(4)	- 58(5)	-20(4)
C(4B)	135(6)	128(5)	165(6)	66(5)	- 33(5)	- 8(4)
C(5B)	168(7)	152(6)	163(6)	82(5)	- 47(5)	-30(5)
C(6B)	164(6)	157(6)	143(5)	88(5)	- 54(5)	-33(4)
C(7B)	169(7)	136(6)	152(6)	74(5)	- 63(5)	- 9(4)
C(8B)	213(8)	169(7)	155(6)	101(6)	- 73(6)	-31(5)
C(9B)	209(9)	182(8)	205(8)	77(7)	- 91(8)	-23(6)
C(10B)	229(10)	160(8)	270(11)	84(7)	-135(9)	-10(7)
C(11B)	192(8)	174(7)	188(7)	92(6)	- 94(7)	-27(6)
C(12B)	150(7)	156(7)	204(7)	61(6)	- 65(6)	- 1(5)
C(13B)	128(6)	168(7)	175(6)	77(5)	- 50(5)	-37(5)
C(14B)	196(9)	323(12)	180(7)	145(9)	- 85(7)	-19(7)
C(15B)	201(9)	445(19)	171(8)	194(11)	- 62(7)	-23(10)
C(16B)	236(11)	336(14)	175(8)	197(11)	-104(8)	-70(8)
C(17B)	229(10)	207(9)	249(10)	137(8)	-121(8)	-48(7)
C(18B)	210(8)	195(8)	201(7)	117(7)	- 98(7)	-27(6)

Figure 1. Comparisons of the observed and calculated structure factors (in electrons x 100) for silole dimer based on the parameters shown in Tables 1 - 4

Description and Discussion of Structure

The unit cell contents of crystalline $Si_2C_{36}H_{36}$ (silole dimer) is illustrated (23) in Figure 2. All atoms lie in crystallographic general positions with the cyclobutane ring of each dimer positioned about a center of symmetry at 0,0,0 and 1/2, 0, 1/2, respectively. The two independent dimers are shown in the stereoscopic views in Figures 3 and 4. The numbering scheme is the same in each dimer to facilitate comparisons. Although the cyclobutane has planarity dictated via the center of symmetry, the least-squares plane through the silacyclopent-2-ene ring (Tables 5 and 6) shows that this ring is only approximately planar which is to be expected because one of the double bonds of the silacyclopentadiene has been destroyed on dimerization. The dihedral angles between the cyclobutane ring and the least-squares plane through the ring of silacyclopent-2-ene are about 119° in both dimers.

Examination of the crystal packing arrangement of silole monomer reveals that the phenyl group ($\emptyset_1$ in Figure 5) is rotated counter-clockwise approximately 12° with respect to coplanarity with the five-membered ring. The phenyl group containing C(13) is rotated about the C(6)-C(13) bond in the same sense as in the monomer and such that the dihedral angles between the phenyl group and the five-membered ring are 30° and 13° in dimers A and B, respectively. This difference is probably due to packing forces.

The C(3)-C(7) distance and the two C-C distances within the cyclobutane ring are 1.49, 1.59, and 1.57 Å, respectively, in dimer A, while these three distances are 1.54 Å in dimer B. This probably indicates a significant difference between the dimers, although inaccuracies in the data militate

Figure 2. A stereoscopic view of the silole dimer unit cell. A right-handed coordinate system with the origin in back lower left corner with X-axis toward the viewer

SILOLE UNIT CELL

SILOLE UNIT CELL

Figure 3. A stereoscopic view of silole dimer A

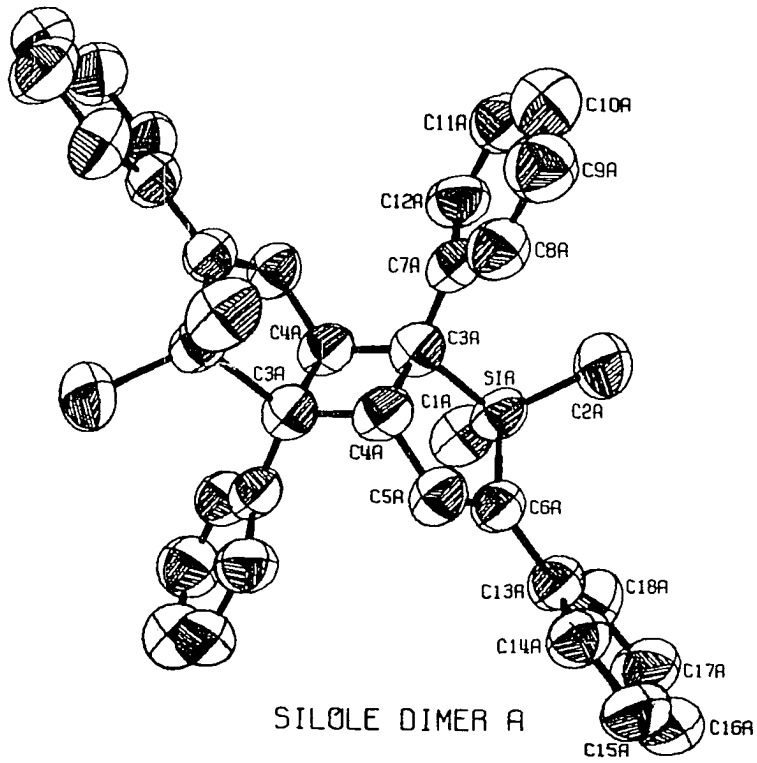

SILOLE DIMER A

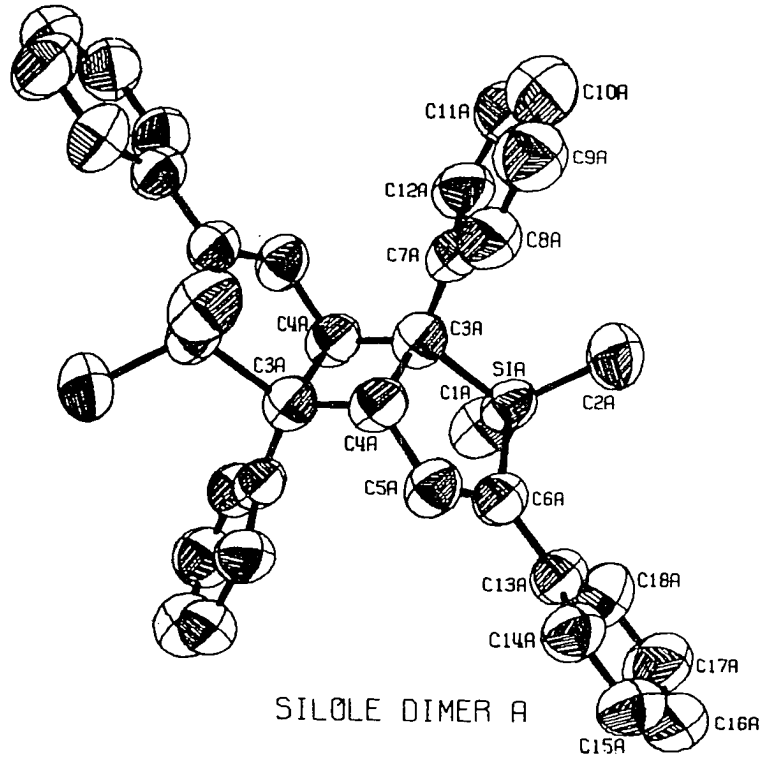

SILOLE DIMER A

Figure 4. A stereoscopic view of silole dimer B

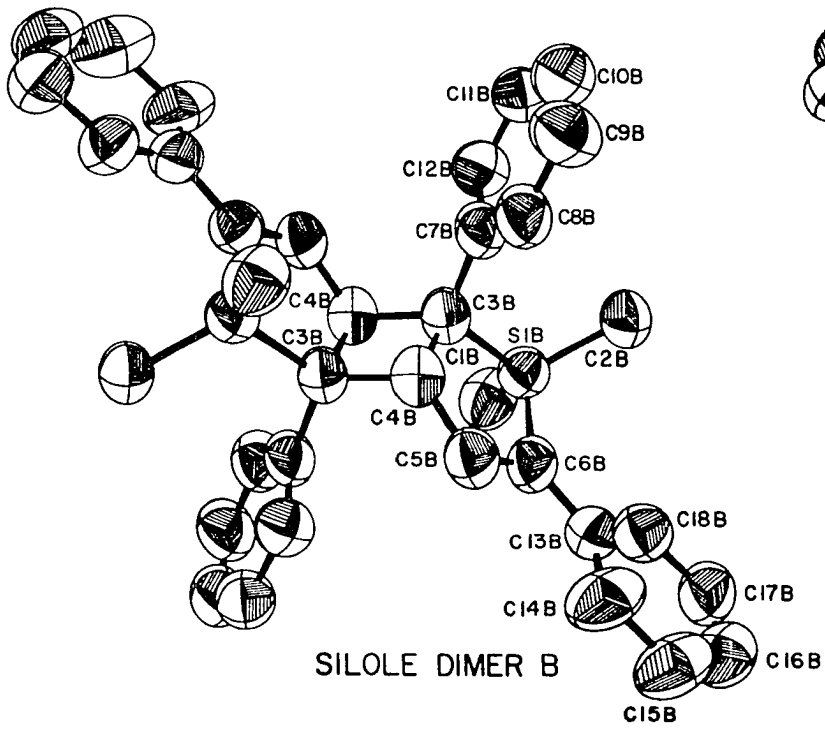

SILOLE DIMER B

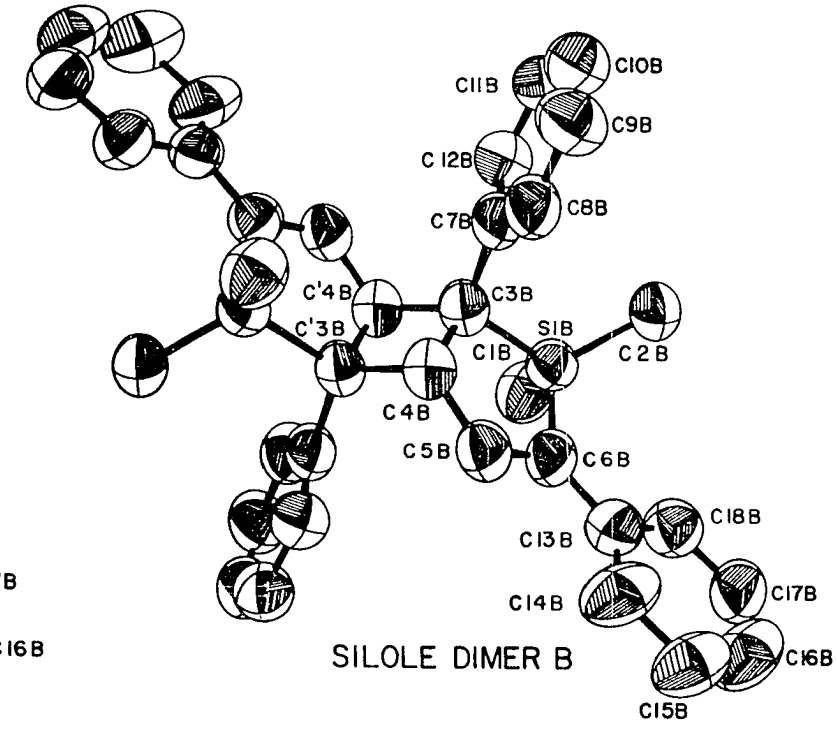

SILOLE DIMER B

Table 5. Equations of some important least-squares planes and distances (Å) of atoms from these planes for dimer A

Plane II	Generated from	Equation
1	C(3A), C(4A), C'(3A), C'(4A)	0.037X +0.913Y -0.405Z -0.0 = 0.0
2	Ø[C(7A) - C(12A)]	-0.617X +0.786Y -0.037Z +0.614 = 0.0
3	Ø[C(13A) - C(18A)]	0.892X +0.208Y -0.401Z -0.570 = 0.0
4	Si(A), C(3A), C(4A), C(5A), C(6A)	-0.633X -0.188Y +0.751Z +0.680 = 0.0
5	C(3A), C(5A), C(7A)	0.725X -0.642Y +0.249Z -0.849 = 0.0

Distances from Plane in Å

Name	(1)	(2)	(3)	(4)	(5)
SiA	-1.670	-1.978	0.660	0.031	1.769
C3A	0.000	-0.137	0.446	-0.067	0.000
C'3A	0.000	1.365	-1.586	1.428	-1.698
C4A	0.000	0.349	-0.326	0.056	-0.868
C'4A	0.000	0.879	-0.815	1.305	-0.830
C5A	-1.162	-0.808	-0.424	-0.005	0.000
C6A	-2.063	-2.009	0.010	-0.040	1.293
C7A	1.116	0.004	1.158	-1.272	0.000
C8A	1.804	-0.016	2.591	-2.499	-0.215
C9A	2.773	0.002	3.842	-3.635	-0.124
C10A	3.051	-0.017	4.384	-3.645	0.281
C11A	2.397	0.006	3.593	-2.459	0.495
C12A	1.402	0.001	2.269	-1.233	0.385
C13A	-3.207	-3.202	-0.011	-0.148	2.214
C14A	-3.112	-3.228	0.008	-0.743	1.856
C15A	-4.190	-4.357	-0.004	-0.840	2.736
C16A	-5.369	-5.496	0.001	-0.389	3.999
C17A	-5.448	-5.465	-0.004	0.189	4.353
C18A	-4.375	-4.343	0.009	0.282	3.476

Table 6. Equations of some important least-squares planes and distances (Å) of atoms from these planes for dimer B

Plane	Generated from	Equation
1	C(3B), C(4B), C'(3B), C'(4B)	0:542X -0.396Y +0.741Z -9.207 = 0.0
2	Ø[C(7B) - C(12B)]	-0.195X +0.928Y -0.317Z +5.750 = 0.0
3	Ø[C(13B) - C(18B)]	0.446X +0.480Y +0.756Z -5.589 = 0.0
4	S(B), C(3B), C(4B), C(5B), C(6B)	0.238X +0.566Y +0.789Z -4.702 = 0.0
5	C(3B), C(5B), C(7B)	0.067X +0.879Y -0.471Z +4.390 = 0.0

Distances from Plane in Å

Name	(1)	(2)	(3)	(4)	(5)
SiB	-1.649	1.990	0.460	-0.026	1.787
C3A	0.000	0.149	0.740	0.049	0.0
C'3B	0.000	-1.332	-0.816	-1.445	-1.650
C4B	0.000	-0.295	0.416	-0.031	-0.858
C'4B	0.000	-0.888	-0.492	-1.365	-0.792
C5B	-1.203	0.869	0.122	-0.014	0.000
C6B	-2.119	2.109	0.148	0.043	1.355
C7B	1.154	0.004	2.147	1.278	0.000
C8B	1.821	0.015	3.214	2.482	-0.286
C9B	2.804	-0.020	4.502	3.613	-0.182
C10B	3.035	0.005	4.693	3.535	0.249
C11B	2.371	0.015	3.653	2.356	0.559
C12B	1.455	-0.020	2.382	1.236	0.387
C13B	-3.258	3.345	0.013	0.203	2.304
C14B	-3.397	3.359	-0.002	0.459	1.898
C15B	-4.489	4.650	-0.012	0.741	2.908
C16B	-5.296	5.771	0.015	0.753	4.198
C17B	-5.199	5.777	-0.003	0.473	4.614
C18B	-4.159	4.535	-0.011	0.183	3.649

Figure 5. A perspective view of the silole monomer packing arrangement. The view corresponds to a right-handed coordinate system with the origin in the back lower left corner and X-axis horizontal

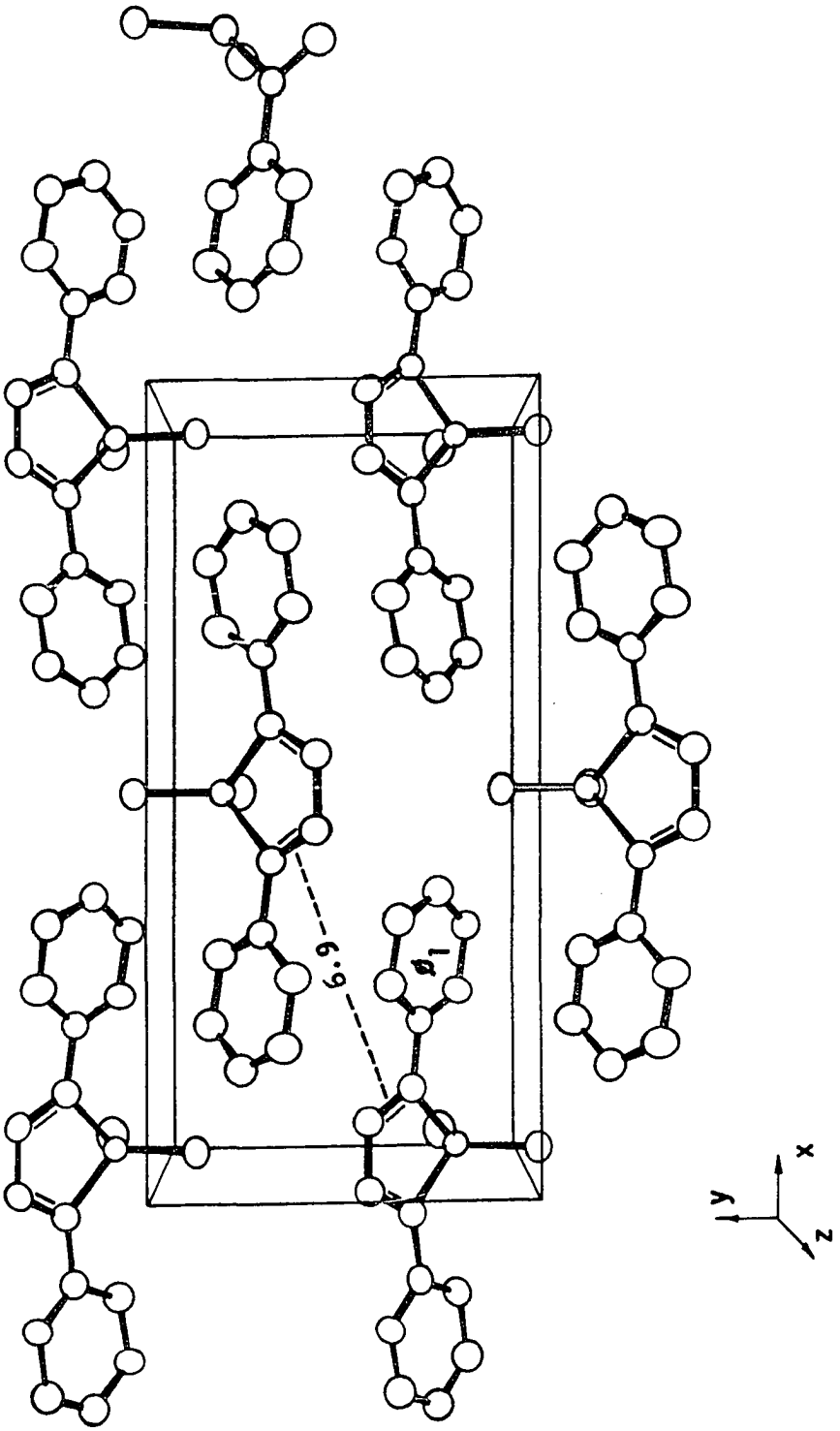
6.9
x
y
z

against forcing this conclusion. However, using mean values gives 1.56 ± 1 Å for the C-C distances in the 4-membered ring, and 1.51 ± 1 Å for C(3)-C(7), which are in substantial agreement with the distances for 1,2,3,4-tetraphenyl-cyclobutane as reported by Dunitz (24). Likewise, the mean Si-C distance of 1.88 ± 1 Å is in substantial agreement with values accepted (25) for this bond type. Selected interatomic distances and angles (26) for the two independent dimers are provided in Tables 7 - 9 while equations of some important least-squares planes and distances of atoms from these planes are given in Tables 5 and 6.

Schmidt (3) has emphasized the importance of short nearest neighbor reactive center ($\rangle C{=}C \langle$) separations in photo-dimerization processes, noting that in either "α-or β-lattices", characterized by centers of symmetry and lattice translations, respectively, reactions failed to proceed if these separations were greater than ~ 4.1 Å. Therefore on this basis, the silole dimer constitutes a violation of the topochemical postulate as formulated by Cohen and Schmidt, because photo-dimerization proceeds through a double bond center to center separation of ~ 6.9 Å and does not occur "with a minimum amount of atomic or molecular movement" (1). Our results indicate that other factors in addition to closeness of nearest neighbor reactive centers are important.

Table 7. Selected interatomic distances[a] in silole dimers A and B, both uncorrected and corrected for thermal motion

Silole Dimer A			Silole Dimer B		
Atoms	uncorr. Å	corr.[b] Å	Atoms	uncorr. Å	corr. Å
Si(A) - C(1A)	1.89	1.91	Si(B) - C(1B)	1.91	1.93
Si(A) - C(2A)	1.85	1.89	Si(B) - C(2B)	1.88	1.90
C(3A) - Si(A)	1.91	1.92	Si(B) - C(3B)	1.91	1.91
C(3A) - C(4A)	1.57	1.58	C(3B) - C(4B)	1.54	1.54
C(3A) - C'(4A)	1.59	1.59	C(3B) - C'(4B)	1.54	1.54
C(4A) - C(5A)	1.51	1.51	C(4B) - C(5B)	1.51	1.51
Si(A) - C(6A)	1.87	1.87	Si(B) - C(6B)	1.85	1.86
C(6A) - C(5A)	1.31	1.32	C(5B) - C(6B)	1.37	1.37
C(3A) - C(7A)	1.49	1.49	C(3B) - C(7B)	1.54	1.54
C(7A) - C(8A)	1.39	1.41	C(7B) - C(8B)	1.41	1.43
C(8A) - C(9A)	1.37	1.39	C(8B) - C(9B)	1.41	1.42
C(9A) - C(10A)	1.37	1.37	C(9B) - C(10B)	1.37	1.37
C(10A) - C(11A)	1.36	1.38	C(11B) - C(10B)	1.40	1.40
C(7A) - C(12A)	1.41	1.43	C(7B) - C(12B)	1.38	1.40
C(11A) - C(12A)	1.43	1.45	C(12B) - C(11B)	1.38	1.39
C(6A) - C(13A)	1.49	1.49	C(6B) - C(13B)	1.48	1.48
C(13A) - C(14A)	1.43	1.45	C(13B) - C(14B)	1.38	1.40
C(14A) - C(15A)	1.39	1.42	C(14B) - C(15B)	1.50	1.51
C(15A) - C(16A)	1.43	1.43	C(16B) - C(15B)	1.34	1.35
C(16A) - C(17A)	1.43	1.45	C(16B) - C(17B)	1.35	1.36
C(13A) - C(18A)	1.42	1.44	C(13B) - C(18B)	1.38	1.41
C(18A) - C(17A)	1.38	1.41	C(17B) - C(18B)	1.44	1.46

[a]All distances have standard deviations of ± 0.01 Å.

[b]The riding model was used to correct for thermal motion, the second atom assumed to ride on the first.

Table 8. Selected interatomic angles[a] in silole dimer A

Atoms	Angle, Deg	Atoms	Angle, Deg
C(2A) - Si(A) - C(6A)	112	C(13A) - C(6A) - Si(A)	127
C(2A) - Si(A) - C(1A)	109	C(8A) - C(7A) - C(12A)	117
C(2A) - Si(A) - C(3A)	114	C(8A) - C(7A) - C(3A)	123
C(6A) - Si(A) - C(1A)	116	C(12A) - C(7A) - C(3A)	120
C(6A) - Si(A) - C(3A)	94	C(9A) - C(8A) - C(7A)	123
C(1A) - Si(A) - C(3A)	112	C(10A) - C(9A) - C(8A)	122
C(7A) - C(3A) - C(4A)	118	C(11A) - C(10A) - C(9A)	117
C(7A) - C(3A) - C'(4A)	118	C(10A) - C(11A) - C(12A)	124
C(7A) - C(3A) - Si(A)	110	C(7A) - C(12A) - C(11A)	117
C(4A) - C(3A) - C'(4A)	88	C(18A) - C(13A) - C(14A)	120
C(4A) - C(3A) - Si(A)	104	C(18A) - C(13A) - C(6A)	120
C'(4A) - C(3A) - Si(A)	115	C(14A) - C(13A) - C(6A)	120
C(5A) - C(4A) - C(3A)	111	C(15A) - C(14A) - C(13A)	119
C(5A) - C(4A) - C'(3A)	121	C(14A) - C(15A) - C(16A)	121
C(3A) - C(4A) - C'(3A)	92	C(15A) - C(16A) - C(17A)	120
C(6A) - C(5A) - C(4A)	120	C(18A) - C(17A) - C(16A)	119
C(5A) - C(6A) - C(13A)	123	C(17A) - C(18A) - C(13A)	122
C(5A) - C(6A) - Si(A)	110		

[a]Estimated standard deviations in all angles are ($\pm$ 1°).

Table 9. Selected interatomic angles[a] in silole dimer B

Atoms	Angle, Deg	Atoms	Angle, Deg
C(2B) - Si(B) - C(6B)	113	C(13B) - C(6B) - Si(B)	127
C(2B) - Si(B) - C(1B)	109	C(8B) - C(7B) - C(12B)	120
C(2B) - Si(B) - C(3B)	114	C(8B) - C(7B) - C(3B)	119
C(6B) - Si(B) - C(1B)	113	C(12B) - C(7B) - C(3B)	121
C(6B) - Si(B) - C(3B)	94	C(9B) - C(8B) - C(7B)	117
C(1B) - Si(B) - C(3B)	115	C(10B) - C(9B) - C(8B)	120
C(7B) - C(3B) - C(4B)	118	C(11B) - C(10B) - C(9B)	124
C(7B) - C(3B) - C'(4B)	117	C(10B) - C(11B) - C(12B)	116
C(7B) - C(3B) - Si(B)	109	C(7B) - C(12B) - C(11B)	123
C(4B) - C(3B) - C'(4B)	92	C(18B) - C(13B) - C(14B)	119
C(4B) - C(3B) - Si(B)	106	C(18B) - C(13B) - C(6B)	119
C'(4B) - C(3B) - Si(B)	115	C(14B) - C(13B) - C(6B)	122
C(5B) - C(4B) - C(3B)	111	C(15B) - C(14B) - C(13B)	120
C(5B) - C(4B) - C'(3B)	120	C(14B) - C(15B) - C(16B)	118
C(3B) - C(4B) - C'(3B)	89	C(15B) - C(16B) - C(17B)	123
C(6B) - C(5B) - C(4B)	120	C(18B) - C(17B) - C(16B)	120
C(5B) - C(6B) - C(13B)	124	C(17B) - C(18B) - C(13B)	120
C(5B) - C(6B) - Si(B)	109		

[a]Estimated standard deviations in all angles are (± 1°).

PART II. CRYSTAL STRUCTURE OF $H_2Ta_6Cl_{18}\cdot 6H_2O$

Introduction

A number of compounds have been reported of the type $[(M_6X_{12})Y_m L_{6-m}]^{(n-m)+}$ where M=Nb, Ta; X=halogen; Y=halogen, L=neutral electron donating ligand such as H_2O; m=number of Y groups, and n=charge on the M_6X_{12} unit. As reported by Burbank (27) and verified by structural information for a number of $M_6X_{12}^{n+}$ containing compounds (27-33) the complex ion $M_6X_{12}^{n+}$ with n=2,3,4 appears to exist as a structural principle in all polynuclear subhalides of the above type, with the tendency to coordinate additional ligands in an octahedral pattern in the solid state. Burbank has further concluded that although four negative ligands consistently coordinate to flatten the M_6 polynucleus, two negative ligands lead to elongation of the M_6 polynucleus, and six negative ligands give rise to an undistorted equilibrium symmetry.

Since the chemistry of polynuclear subhalides is still in its formative stage, we felt that structural information of another $M_6X_{12}^{n+}$ containing compound would be of interest. Therefore we undertook an X-ray study of $H_2Ta_6Cl_{18}\cdot 6H_2O$ for which n=4.

Experimental

A sample of the compound was kindly supplied by Dr. R. E. McCarley and dark red crystals were obtained by recrystallization from a hydrochloric acid solution through which chlorine gas had been passed. Microscopic examination revealed that the crystals were octahedral with sharply defined edges. Crystals were selected and mounted in thin-walled Lindemann glass capillaries to prevent decomposition in the atmosphere. Pre-

liminary precession photographs exhibited m3m symmetry indicating a cubic space group. The conditions limiting the possible reflections were hkl when $h+k=2n$ ↻, hhl when $l+h=2n$ ↻, 0kl when $k+l=4n$, $(k,l=2n)$ ↻, and hkl when $h+k+l=2n+1$ or $4n$. These conditions are consistent with space group $Fd3m(O_h^7)$. The unit cell parameter at $23\pm3^{\circ}C$ is $a = 19.92\pm1$ Å, as determined by a least-squares fit to 13 independent reflection angles whose centers were determined by left-right, top-bottom beam splitting on a previously aligned General Electric XRD-5 counter diffractometer (Mo K_α radiation, $\lambda = 0.7107$ Å). The unit cell was assumed to contain eight molecules of $H_2Ta_6Cl_{18}\cdot 6H_2O$ leading to a calculated density of 3.08 g/cm^3 which is in reasonable agreement with the expected value.

For data collection, a crystal having approximate dimensions 0.10 x 0.10 x 0.086 mm along the a, b, c crystal axes, respectively, was mounted such that the 0.086 mm axis was along the spindle axis.

Data were collected at room temperature ($23 \pm 3^{\circ}$ C) utilizing a General Electric XRD-5 diffractometer equipped with a scintillation counter and using zirconium filtered molybdenum Kα radiation ($\lambda = 0.7107$ Å). Within a two theta sphere of 50°, all data in 1/6 of an octant ($h \geq k \geq l$) were recorded using the $\theta - 2\theta$ scan technique with a take-off angle of 3°. A symmetric scan range of 3.33° in 2θ was used and stationary-crystal, stationary-counter background counts were made at each end of the scan. Counting times for the latter were 20 sec, if $2\theta \geq 15^{\circ}$ and 40 sec if $2\theta < 15^{\circ}$. The scan rate was 2°/min. A total of 365 reflections were measured in this way.

As a general check on electronic and crystal stability, the intensities of three standard reflections (642, 911, and 800) were remeasured

periodically during the data collection period. These reflections decreased slowly in intensity, the total decrease being about 6.5% during the entire period of data collection; such a decrease was considered quite acceptable and the data were appropriately corrected.

The intensity data were also corrected for Lorentz-polarization effects and for effects due to absorption. The absorption coefficient, μ, is 194.49 cm^{-1}, and an absorption correction was made using a computer program by Wehe, et al. (34). The maximum and minimum transmission factors were 26.6% and 29.4% respectively. Of the 365 measured intensities, 214 were found to be above background, (i.e., greater than three times the standard error based on counting statistics) and therefore considered as observed. The unobserved reflections were not used in the solution and refinement of the derived structure.

The estimated error in each intensity measurement was calculated by

$$[\sigma(I_o)]^2 = [C_t + J*C_b + (K_t*C_t)^2 + (K_b*J*C_b)^2 + (K_a*C_r)^2]/(A*Lp)^2$$

where J is 5/2 or 5/4 depending on whether background counts were measured for 20 sec or 40 sec, respectively, and where C_t and C_b are the total count and the background count, respectively. Also $C_r = C_t - J*C_b$, A is the transmission factor, and K_t, K_b, and K_a are the fractional random errors in C_t, C_b, and A, respectively. A value of 0.04 was arbitrarily assigned to K_t, K_b, and K_a. The estimated standard deviation in each structure factor was calculated by

$$\sigma(F_o) = [(I_o) + \sigma(I_o)]^{\frac{1}{2}} - |F_o|,$$

a function based on the finite difference method (18). These standard deviations were used during the least-squares refinements to weight the observed structure factors where w, the individual weighting factor,

Table 10. Final values of the positional parameters and their standard deviations[a] for $H_2Ta_6Cl_{18}\cdot 6H_2O$

Atom	Position	X/a	Y/b	Z/c
Ta	48f	0.23016(7)	0.125	0.125
Cl(term.)	48f	0.35606(46)	0.125	0.125
Cl(bridg.)	96g	0.12543(47)[b]	Z/c	0.24526(22)

[a]Numbers in parentheses represent standard deviations occurring in the last digit of the parameter.

[b]This bridging chlorine position is within a standard deviation of the symmetry fixed position, 0.125.

was defined as $1/\sigma(F_o)^2$.

Solution and Refinement of Structure

Examination of the Patterson function readily revealed trial positions for the tantalum cluster. The positions were then refined by full-matrix least-squares methods with isotropic thermal parameters to a conventional discrepancy factor of $R = \Sigma||F_o| - |F_c||/\Sigma|F_o| = 0.135$ and a weighted R-factor of $_wR = (\Sigma w(|F_o| - |F_c|)^2/\Sigma w|F_o|^2)^{\frac{1}{2}} = 0.143$. The scattering factors used were those of Cromer and Waber (22) with modifications for the real and imaginary parts of anomalous dispersion (35).

A difference electron density map (36) at this stage showed that apparently all atoms had been accounted for, but that some anisotropic motion, particularly of the heavier atoms, was quite evident.

After adding the ten anisotropic thermal parameters allowed by symmetry (37), there were a total of 15 parameters to be varied and therefore, 13 reflections/variable. Therefore, full-matrix anisotropic least-squares refinement was considered justified.

Final values of R and $_wR$ of 0.053 and 0.055, respectively, were obtained. Even though no oxygen atoms had been added to the refinement, a final difference electron density map was calculated and exhibited no peak above one electron/Å^3 in any chemically reasonable position. Therefore, the water molecules were assumed to be disordered.

In Table 10 are given the final values of the positional parameters, along with their standard deviations as derived from the inverse matrix of the last cycle of the least-squares refinement. In Figure 6 are given the values of F_o and F_c in electrons for the 214 reflections above back-

Figure 6. Comparison of observed and calculated structure factors (in electrons) for $H_2Ta_6Cl_{18}\cdot 6H_2O$ based on the parameters shown in Tables 10 and 11

H = 1

K	L	FO	FC
1	1	2186	-2577

H = 2

K	L	FO	FC
2	0	1598	-1482

H = 3

K	L	FO	FC
1	1	839	-746
3	1	249	-279
3	3	969	-676

H = 4

K	L	FO	FC
0	0	1434	-1382
2	2	688	-682
4	0	712	-602
4	4	650	871

H = 5

K	L	FO	FC
1	1	434	342
3	1	535	-518
3	3	841	805
5	1	689	738
5	3	1052	971
5	5	1225	-1152

H = 6

K	L	FO	FC
2	0	319	349
4	2	1265	1273
6	0	392	505
6	4	1792	-1758

H = 7

K	L	FO	FC
1	1	1248	1240
3	3	708	785
5	1	316	317
5	3	949	-965
5	5	1113	-1126
7	1	343	389
7	3	543	-547
7	5	765	764
7	7	327	212

H = 8

K	L	FO	FC
0	0	3409	3622
2	2	669	-713
4	0	450	-594
4	4	958	-927
6	6	761	742
8	0	2346	2375
8	8	1690	1583

H = 9

K	L	FO	FC
1	1	1861	-1960
3	1	775	-748
3	3	111	-44
5	1	410	414
5	3	288	-272
5	5	492	478
7	1	1079	1106
7	3	219	-144
7	5	43	108
7	7	506	490
9	1	1562	-1593
9	3	769	-711
9	5	475	442
9	7	990	960
9	9	1376	-1335

H = 10

K	L	FO	FC
2	0	1675	-1739
4	2	147	100
6	0	862	894
6	4	418	431
8	2	1097	-1098
8	6	459	449
10	0	1686	-1768
10	4	481	475
10	8	1269	-1230

H = 11

K	L	FO	FC
1	1	1011	-981
3	1	268	287
5	3	258	246
5	5	314	388
7	1	455	-409
7	3	152	134
7	5	315	-309
9	1	881	-896
9	3	329	318
9	5	115	135
9	7	456	-430
9	9	827	-806
11	1	516	521
11	3	194	178
11	5	110	-70
11	7	242	-195
11	9	479	472
11	11	341	324

H = 12

K	L	FO	FC
0	0	1165	-1226
2	2	82	66
4	4	371	399
6	2	430	404
6	6	795	-790
8	0	749	-731
8	4	212	-266
8	8	404	-382
10	2	422	408
10	6	62	-20
10	10	636	581
12	0	258	303
12	4	88	63
12	12	187	-164

H = 13

K	L	FO	FC
1	1	346	322
3	1	127	-149
3	3	360	351
5	1	313	314
5	3	510	508
5	5	667	-650
7	3	453	-454
7	5	582	-579
7	7	399	380
9	1	344	334
9	3	139	-69
9	5	234	205
9	7	116	-7
9	9	333	343
11	1	209	157
11	3	71	28
11	5	167	148
11	7	138	-101
11	9	188	163
11	11	180	-160
13	1	73	110
13	3	265	262
13	5	351	-363
13	7	322	-297
13	9	58	59
13	11	142	43
13	13	146	-194

H = 14

K	L	FO	FC
2	0	53	69
4	2	834	795
6	0	399	422
6	4	1153	-1122
8	2	169	-178
8	6	563	567
10	0	416	416
10	4	364	322
10	8	211	171
12	2	315	290
12	6	224	-544
12	10	42	25
14	0	305	362
14	4	777	-778
14	8	440	447
14	12	384	-396

H = 15

K	L	FO	FC
1	1	308	308
3	1	294	290
3	3	695	681
5	1	460	451
5	3	828	-803
5	5	925	-900
7	3	581	-549
7	5	673	686
7	7	330	385
9	1	319	356
9	5	257	292
9	9	364	349
11	3	256	257
11	5	391	-372
13	3	450	-451
13	5	529	-519
13	7	393	403
13	13	299	-296
15	3	477	-492
15	5	560	585
15	7	406	403

H = 16

K	L	FO	FC
0	0	1192	1219
4	0	184	191
4	4	1015	-1022
6	2	474	-494
6	6	832	830
8	0	806	801
8	4	323	346
8	8	520	497
10	2	256	-254
10	10	442	-436
12	0	183	-88
12	4	463	-494
14	2	388	-401
14	6	670	615
16	0	162	203
16	4	405	448

H = 17

K	L	FO	FC
1	1	780	-773
3	3	258	-241
5	3	315	-371
5	5	470	486
7	1	410	411
7	5	241	243
9	1	685	-674
9	3	231	-226
9	7	355	372
9	9	669	-599
11	1	313	-358
11	9	372	-343
13	5	253	273
15	1	150	100

H = 18

K	L	FO	FC
2	0	910	-913
6	0	488	490
8	2	610	-606
10	0	910	-950
10	4	218	234
10	8	682	-679
14	0	197	234

H = 19

K	L	FO	FC
1	1	619	-646
3	1	255	295
7	1	317	-355
9	1	580	-581
9	3	268	276
9	7	347	-335
9	9	485	-521
11	1	396	377
11	9	355	329

H = 20

K	L	FO	FC
0	0	785	-822
2	2	299	312
8	0	553	-569
8	8	380	-376
10	2	419	412
12	0	354	339

H = 21

K	L	FC	FC
1	1	340	309

H = 22

K	L	FO	FC
2	0	239	180
6	0	210	51
6	4	369	-351

H = 23

K	L	FO	FC
5	3	327	-335

H = 24

K	L	FO	FC
0	0	310	318

Table II. Final values of the thermal parameters[a] and their standard deviations[b] for $H_2Ta_6Cl_{18}\cdot 6H_2O$

Atom	Position	β_{11}	β_{22}	β_{33}	β_{12}	β_{13}	β_{23}
Ta	48f	172(5)	193(3)	β_{22}	0.0	0.0	4(5)
Cl(term.)	48f	213(26)	337(20)	β_{22}	0.0	0.0	13(35)
Cl(bridg.)	96g	314(20)	β_{33}	203(9)	β_{13}	28(14)	-29(12)

[a]The form of the anisotropic temperature factor expression is $\exp[-(\beta_{11}h^2 + \beta_{22}k^2 + \beta_{33}l^2 + 2\beta_{12}hk + 2\beta_{13}hl + 2\beta_{23}kl)]$.

[b]Numbers in parentheses are standard deviations occurring in the last digit of the parameter.

ground. The values of F_c for unobserved reflections in no case exceeded $3\sigma(F_o)$. An indication of the directions and root-mean square amplitudes of vibration for the atoms refined anisotropically is provided by Table II.

Description and Discussion

The unit cell of crystalline $H_2Ta_6Cl_{18}\cdot 6H_2O$ showing only the $Ta_6Cl_{18}^{=}$ anions is illustrated (23) in Figure 7. The tantalum and terminal chlorine atoms lie in positions of mm crystallographic symmetry, while the bridging chlorines lie on mirror planes. The effect is to give a cell consisting of eight distinct and regular octahedral $Ta_6Cl_{18}^{=}$ anion clusters (O_h symmetry), with centers at: (1/8, 1/8, 1/8), (1/8, 5/8, 5/8), (5/8, 5/8, 1/8), (5/8, 1/8, 5/8), as well as others related to these by the center of symmetry. Also there are 'holes' ($\sim$ 9 Å diameter) in the structure with centers at: (3/8, 3/8, 3/8), (1/8, 5/8, 1/8), (5/8, 1/8, 1/8), (1/8, 1/8, 5/8), plus others related to these by the center of symmetry. This arrangement of tantalum clusters and 'holes' is that of two interpenetrating diamond type lattices, respectively. The $Ta_6Cl_{18}^{=}$ ion cluster is stereoscopically shown in Figure 8.

Comparison of van der Waals' contacts between clusters and intracluster distances is provided in Table 12. Bond lengths, both uncorrected for thermal motion and corrected using the riding model approximation are given in Table 13. The terminal Ta-Cl distance of 2.507 $\pm$ 9 Å is significantly longer than the bridging Ta-Cl distance of 2.414 $\pm$ 5 Å, and such a lengthening is in agreement with other polynuclear subhalides (29-33). The Ta-Ta distance of 2.962 $\pm$ 2 Å as well as bridging and terminal Ta-Cl distances in the $Ta_6Cl_{18}^{=}$ cluster compare favorably with the

Figure 7. A stereoscopic view of the packing of $Ta_6Cl_{18}^{=}$ anion clusters in the unit cell. The view corresponds to a right-handed coordinate system with the origin in the front lower left corner with the X-axis horizontal

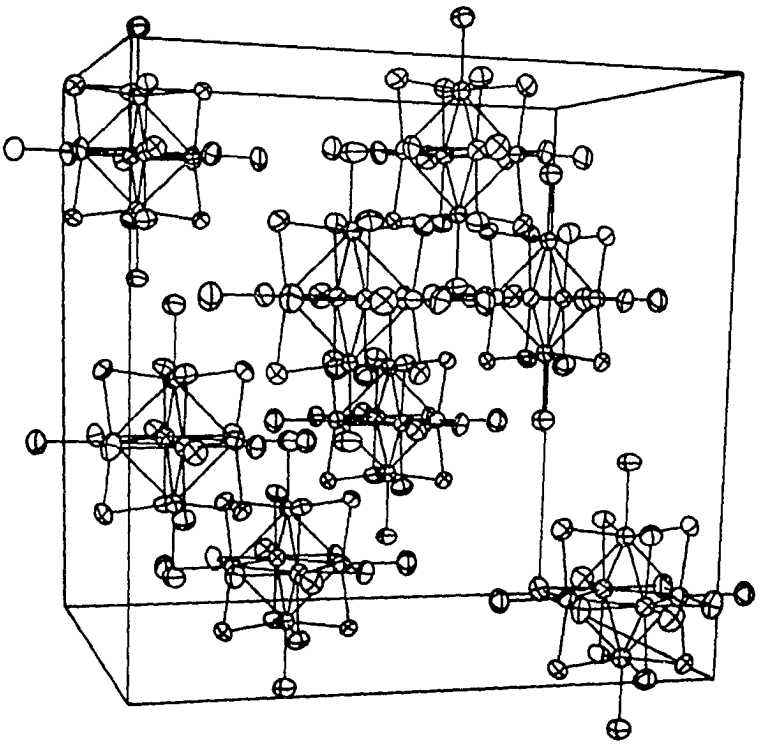

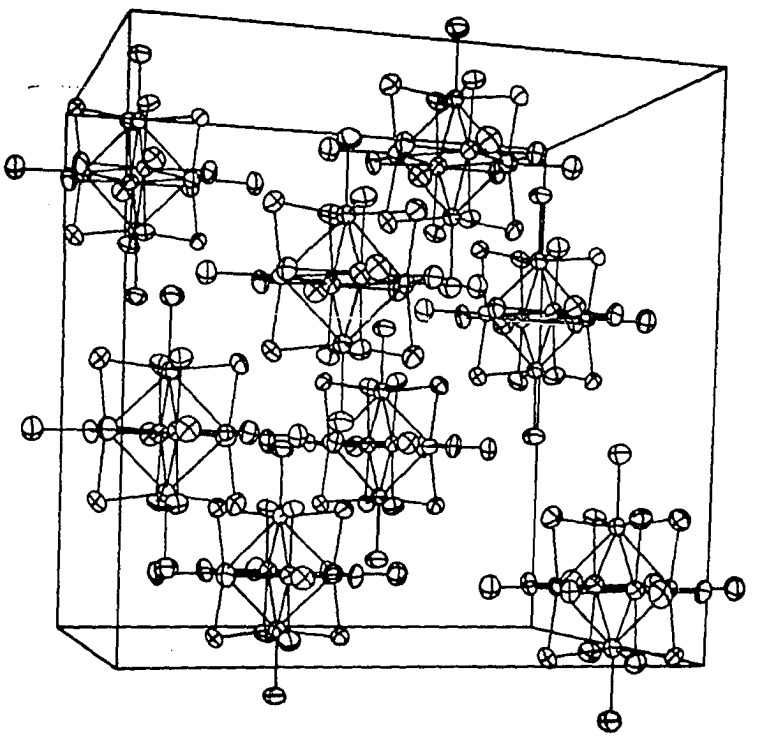

Figure 8. A stereoscopic view of the $Ta_6Cl_{18}^{=}$ anion cluster

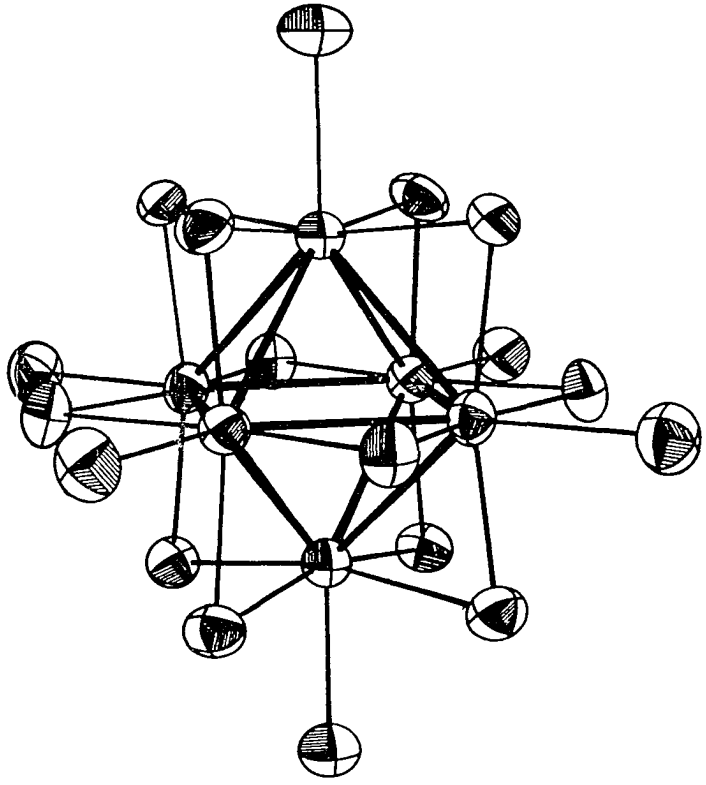

TANTALUM CHLORIDE CAGE COMPOUND

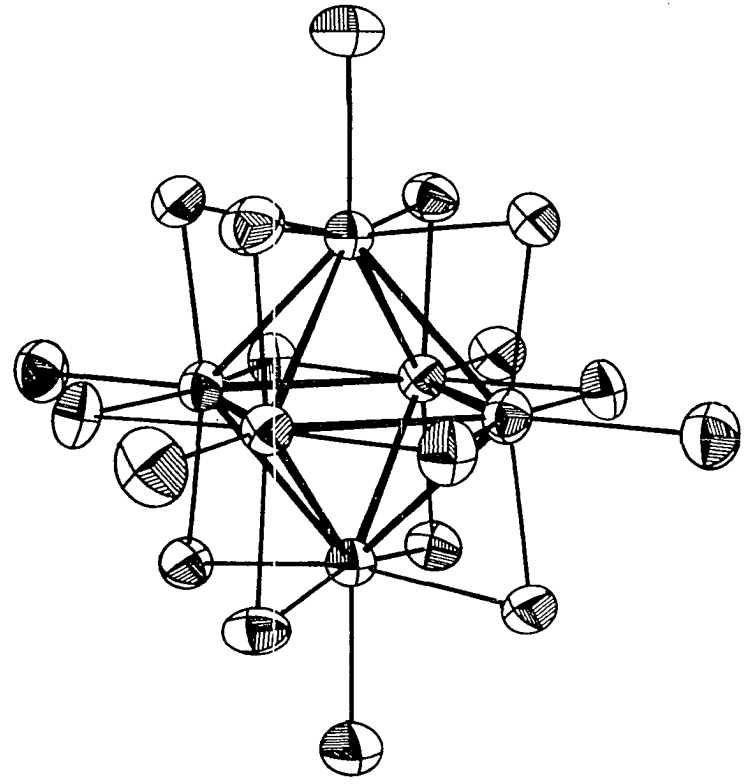

TANTALUM CHLORIDE CAGE COMPOUND

Table 12. Comparison of van der Waals contacts between $Ta_6Cl_{18}^{=}$ clusters and intracluster distances[a], and their associated standard deviations[b]

Atoms	Length, Å Between Clusters	Length, Å in Same Cluster
Cl(term)-Cl(bridg)	3.675(0.006)	3.250(0.008)
Cl(bridg)-Cl(bridg)	3.671(0.013)	3.384(0.017)
Cl(term)-Cl(term)	5.007(0.003)	6.499(0.017)

[a]All distances are uncorrected for thermal motion.

[b]Numbers in parentheses refer to the standard deviations in the last digit.

Table 13. Comparison of bond lengths using the riding model approximation to the correction for thermal motion[a]

Bond	Length, Å (Uncorr)	Length, Å (Riding-Motion)[b]
Ta-Cl(term)	2.507(0.009)	2.519(0.009)
Ta-Cl(bridg)	2.414(0.005)	2.421(0.005)
Ta-Ta	2.962(0.002)	2.962(0.002)

[a]Numbers given in parentheses refer to the standard deviations occurring in the last digit.

[b]Second atom assumed to ride on the first.

Table 14. Compilation of some distances[a] in $[(M_6X_{12})Y_mL_{6-m}]^{(n-m)+}$

Compound	d(M-M), Å		d(M-X), Å	d(M-Y), Å	d(X-X), Å
Ta_6I_{14} (28)	2.805 3.080	2.90[b]	2.754		3.785
$Ta_6Cl_{14}\cdot 7H_2O$ (27)	2.96				
Ta_6Cl_{15} (29)	2.925		2.434	2.564	3.408
$H_2Ta_6Cl_{18}\cdot 6H_2O$	2.962		2.414	2.507	3.384
Nb_6Cl_{14} (30)	2.895 2.955	2.915[b]	2.407	2.58	3.385
$K_4(Nb_6Cl_{18})$ (31)	2.915		2.49	2.596	3.47
Nb_6F_{15} (32)	2.80		2.05	2.11	2.89
$[(CH_3)_4N]_2Nb_6Cl_{18}$ (33)	3.02		2.42	2.46	3.40

[a]All distances refer to average values.

[b]Tetragonal flattening.

structural data about other $[(M_6X_{12})Y_mL_{6-m}]^{(n-m)+}$ species, as indicated in Table 14. A comparison of the results in this table shows that there is a consistent lengthening of the M-M distance upon oxidation of the $M_6X_{12}^{n+}$ cluster. The M-Y (terminal) distance is also shortened upon oxidation of the $M_6X_{12}^{n+}$ cluster and is shorter than one would expect after equilibration of the intracluster repulsion forces due to lengthening of the M-M distance. Our results appear reasonable in view of molecular orbital studies of the $M_6X_{12}^{n+}$ species (38, 39). Infrared spectra of these polynuclear subhalides with $\underline{n}$ = 3,4 have been interpreted on the basis of tighter binding in the M-Y (terminal) bond (40).

It would be reasonable to assume that the six waters and two protons reside in the approximately 9 Å 'holes' in the structure, but with no preferred ordering. This would account for the fact that there were no peaks found on the difference map above a value of 1 electron/Å^3, although no oxygen atoms had been included in the structure factor calculation.

In $(HNb_6I_8)^{3+}$ (41), the hydrogen atom was found to reside in the center of the Nb_6 cluster, but chemical evidence (42) seems to rule out a similar position for the proton in this case.

PART III. A TECHNIQUE FOR COOLING SINGLE CRYSTALS BELOW 90°K FOR X-RAY DIFFRACTION

Introduction

In recent years a number of low temperature systems for single crystal X-ray diffraction investigations have been reported in the literature. The recent systems have in general incorporated elaborate electronic level controlling devices or some type of pressure control to maintain constant pressure of the outflowing gas (43, 44). These systems have the disadvantage of having a large number of components and tend to be expensive. We have developed a crystal cooling apparatus that incorporates many of the features of systems recently developed, but uses a level controller consisting of a float and microswitch arrangement in a miniature Dewar and a gravity feed intermediate Dewar system to reduce pressure variations.

Description and Operation

The apparatus consists of three Dewars and associated electronics as shown in Figure 9. Liquid nitrogen is boiled from the small Dewar to provide the cold gas stream for cooling the crystal. The small size of the Dewar allows placement of this vessel close to the crystal and permits the use of a short delivery nozzle which is usually positioned 2-3 mm from the crystal. The miniature Dewar is silvered except for a narrow strip along the side which permits inspection of the components inside. A heater (wire wound resistor, 250Ω, 10W) is used to provide the constant flow of cold gas via boiling liquid nitrogen. As the liquid level in the miniature Dewar falls, a microswitch is triggered and a magnetic valve is energized which permits liquid nitrogen to gravity-feed from the inter-

Figure 9. Diagram showing miniature Dewar and auxiliary apparatus

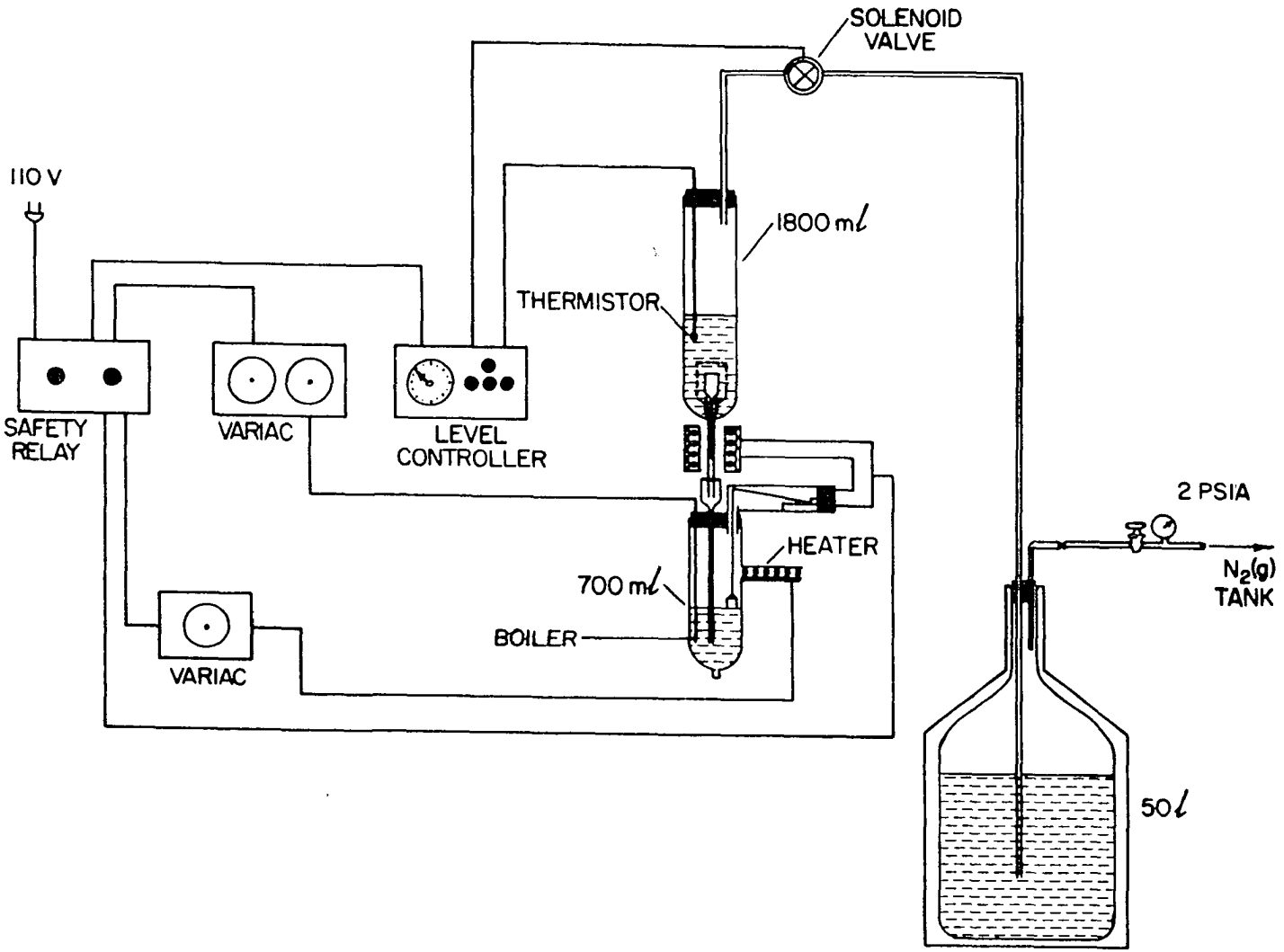
SOLENOID VALVE
110 V
1800 mℓ
THERMISTOR
SAFETY RELAY
VARIAC
LEVEL CONTROLLER
2 PSIA
HEATER
N_2(g) TANK
700 mℓ
BOILER
VARIAC
50 ℓ

Figure 10. Diagram showing details of miniature and intermediate Dewars

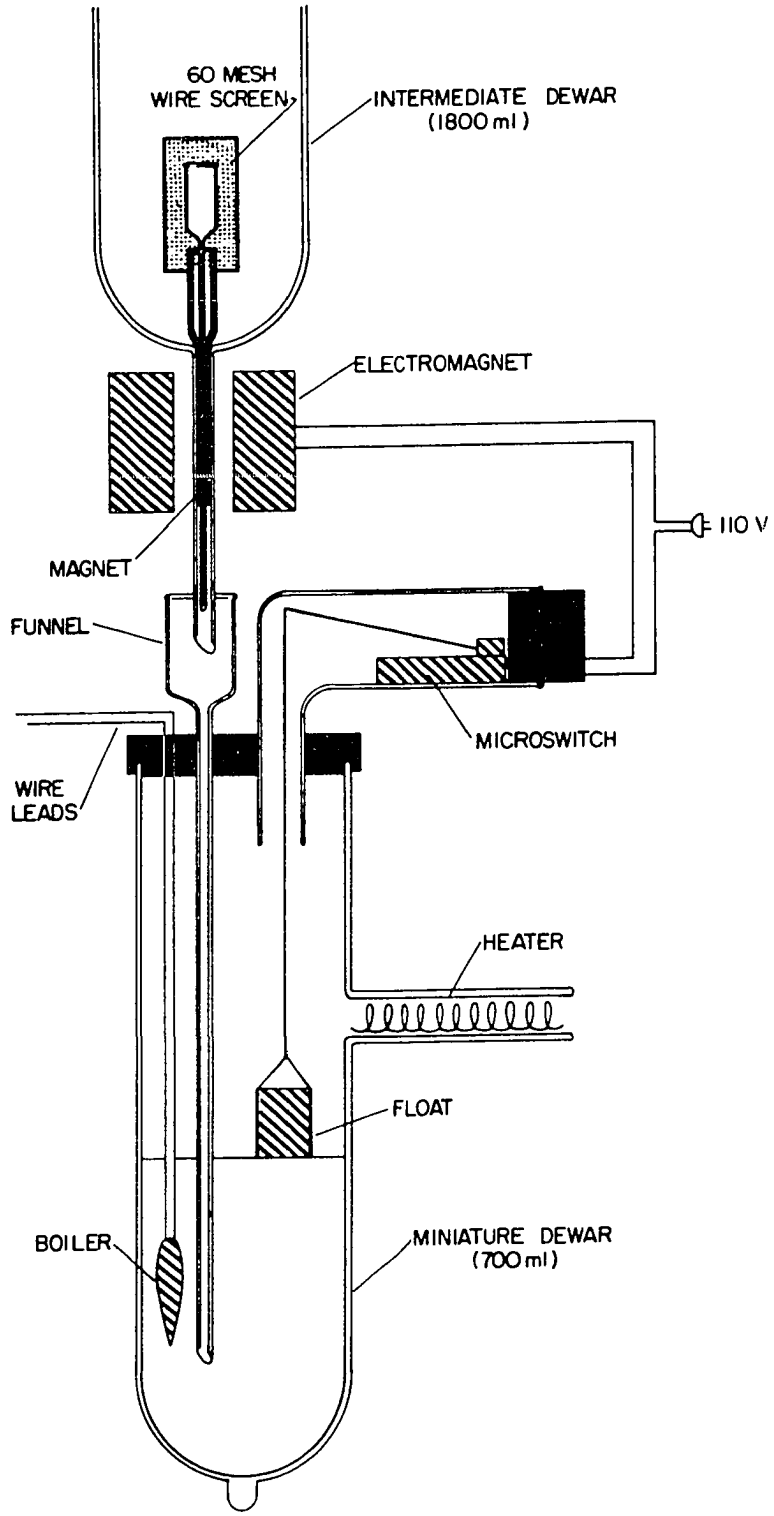
60 MESH
WIRE SCREEN
INTERMEDIATE DEWAR
(1800 ml)
ELECTROMAGNET
110 V
MAGNET
FUNNEL
MICROSWITCH
WIRE
LEADS
HEATER
FLOAT
BOILER
MINIATURE DEWAR
(700 ml)

mediate Dewar to the small Dewar (Figure 10). A small float is used in triggering the microswitch. By using such a float we find that the liquid nitrogen level in the small Dewar can be kept constant to with $\pm$ 5 mm. Since the level is kept constant and since refilling takes place by a gravity mechanism, the gas pressure remains essentially constant and hence a fine temperature control can be attained.

The intermediate Dewar is refilled from a 50 liter supply Dewar. A commercial electronic level controller (Cryogenic Associates, Inc.) is used to trigger the refilling action, although other devices could also be readily employed for this purpose. As the liquid level falls below the thermistor (level sensor), the level controller energizes a solenoid valve and liquid nitrogen flows for a preset time from the pressurized reservoir (2 PSI). If a malfunction occurs (i.e. empty reservoir, microswitch failure, etc.) a safety relay turns off the system.

We have found, as have Abowitz and Ladell (43), that a fine mesh stainless steel screen (400 x 2500 mesh, Unique Wire Weaving Co.) placed over the inlet hole of the delivery nozzle prevents powdered ice particles which are often in the liquid nitrogen from being carried along in the gas stream to the crystal. Ice formation at the cold gas exit can be effectively eliminated by using a resistance heater attached around the exit by means of a silicone adhesive (General Electric Co.).

Results

The temperature of the cold gas stream was monitored by means of a copper-constantan thermocouple placed approximately 2 mm from the exit point, outside the delivery nozzle. The thermocouple wire leads were run

Figure 11. Gas temperature at outlet of delivery nozzle versus consumption of liquid nitrogen

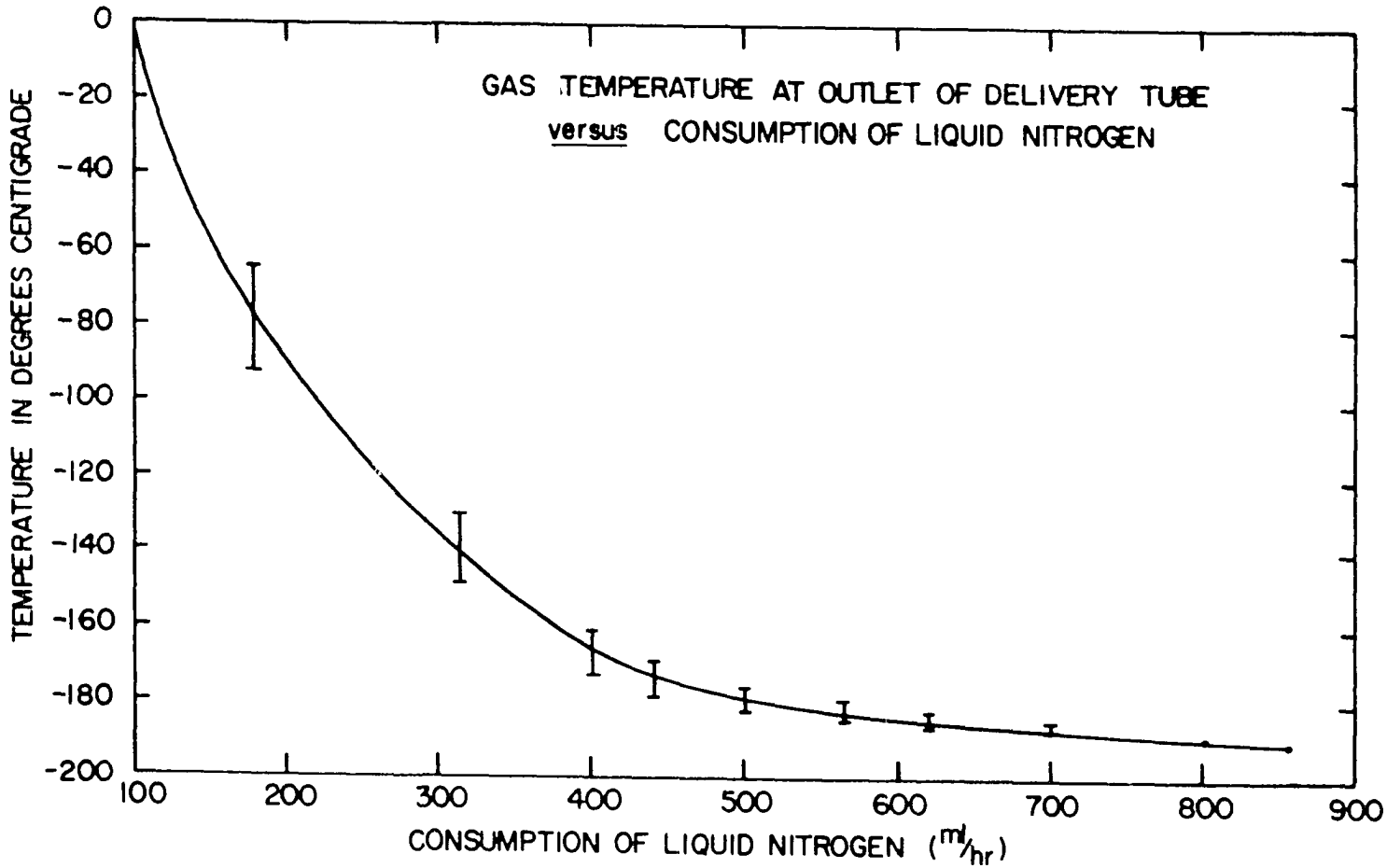
GAS TEMPERATURE AT OUTLET OF DELIVERY TUBE
versus CONSUMPTION OF LIQUID NITROGEN
TEMPERATURE IN DEGREES CENTIGRADE
0
-20
-40
-60
-80
-100
-120
-140
-160
-180
-200
100
200
300
400
500
600
700
800
900
CONSUMPTION OF LIQUID NITROGEN (ml/hr)

through the length of the nozzle to minimize any temperature gradients.

The temperature of the gas stream impinging on the crystal in our system can be controlled by either of two methods: (1) the rate of cold gas flow can be varied, or (2) the amount of current in a heater placed in the delivery nozzle can be varied. Figure 11 shows results obtained with the first method. It should be noted, as would be expected, that the first method does not give fine temperature control except at higher flow rates. Therefore we generally operate in the second mode, use a higher flow rate (e.g. 850 ml/hr) and use the nozzle heater (open helix of resistance wire) to maintain temperatures at the crystal to within $\pm$ 0.5°C of the desired temperature between ambient and -192°C.

Discussion

Although fine temperature control is not essential for low temperature data collection (45) it is nonetheless a very desirable feature, especially if one wishes to grow single crystals *in situ* from the melt at temperatures below room temperature. By maintaining essentially a constant liquid level and by using a gravity-feed instead of a pressure-feed mechanism, we have obtained fine temperature control; yet our system is relatively inexpensive compared with other systems, particularly those which control the pressure of the effluent gas directly (43).

The small size of the miniature Dewar permits its being positioned directly on a diffractometer. In the course of a recent investigation at *ca.* -187°C liquid nitrogen was consumed at the rate of less than 20 liters per day (46).

SUMMARY AND CONCLUSIONS

The crystal structure of 1,1-dimethyl-2,5-diphenyl-1-silacyclopentadiene photodimer (silole dimer) has been determined, and the counter intensity data have been refined by anisotropic least-squares analysis. The silole dimer molecule contains a completely planar cyclobutane ring via the center of symmetry. The mean C-C distance within this 4-membered ring is 1.56 Å and is probably longer than the normal C-C single bond length. The mean Si-C distance is 1.88 Å. Elucidation of the structure of silole dimer establishes the path of approach producing the photoproduct as being between two photo active monomers related by a screw axis with a reactive center distance of ~ 6.9 Å. The principle feature of this reaction system is that it constitutes a significant departure from the "topochemical" postulate as formulated by Cohen and Schmidt.

The crystal structure of $H_2Ta_6Cl_{18}\cdot 6H_2O$ has been determined, and the three-dimensional scintillation counter data refined by anisotropic least-squares analysis. The structure is cubic and consists of $Ta_6Cl_{18}^{=}$ anion clusters of O_h symmetry, which pack in a diamond type lattice. The Ta-Ta distance is 2.962 Å. The terminal Ta-Cl distance 2.507 Å is significantly longer than the bridging Ta-Cl distance of 2.414 Å.

An efficient and inexpensive method of cooling a crystal to low temperatures and maintaining fine temperature control at the crystal has been developed for single crystal X-ray diffraction investigations. The principal features of this system are the use of a float and microswitch mechanism to maintain a virtually constant liquid level in the boil-off

chamber, and the use of a slow gravity fill procedure to reduce any pressure variations in the gas stream. Operation of the cooling system at $\sim 90^{\circ}K$ requires less than 20 liters of liquid nitrogen per day.

LITERATURE CITED

1. Cohen, M. D. and Schmidt, G. M. J., J. Chem. Soc., 1996 (1964).

2. Cohen, M. D., Schmidt, G. M. J., and Sonntag, F. I., J. Chem. Soc., 2000 (1964).

3. Schmidt, G. M. J., J. Chem. Soc., 2014 (1964).

4. Bregman, J., Osaki, K., Schmidt, G. M. J., and Sonntag, F. I., J. Chem. Soc., 2021 (1964).

5. Rabinovich, D. and Schmidt, G. M. J., J. Chem. Soc., 2030 (1964).

6. Cohen, M. D., Schmidt, G. M. J., and Flavian, S., J. Chem. Soc., 2041 (1964).

7. Cohen, M. D., Hirshberg, Y., and Schmidt, G. M. J., J. Chem. Soc., 2051 (1964).

8. Cohen, M. D. Hirshberg, Y., and Schmidt, G. M. J., J. Chem. Soc., 2060 (1964).

9. Bregman, J., Leiserowitz, L., and Schmidt, G. M. J., J. Chem. Soc., 2068 (1964).

10. Bregman, J., Leiserowitz, L., and Osaki, K., J. Chem. Soc., 2086 (1964).

11. Barton, T. J., Ames, Iowa. Photo-dimerization of silole monomer in solid state. Private communication. 1969.

12. Clardy, J. C. and Read, L., Ames, Iowa. Data concerning silole monomer. Private communication. 1969.

13. Barton, T. J. and Nelson, A. J., Tetrahedron Letters, 57, 5037 (1969).

14. Howells, E. R., Philips, D. C., and Rodgers, D., Acta Cryst., 3, 210 (1950).

15. Lawton, S. L. and Jacobsen, R. A., The reduced cell and it's crystallographic applications. U.S. Atomic Energy Commission Report IS-1141 (Iowa State University of Science and Technology, Ames, Institute for Atomic Research), 1965, Chapter 3, p. 108.

16. Williams, D. E. A fortran lattice constant refinement program. U.S. Atomic Energy Commission Report IS-1052 (Iowa State University of Science and Technology, Ames, Institute for Atomic Research). 1964.

17. Ahmed, F. R. and Singh, P. Absorption correction for the 3-circle goniostat geometry. National Research Council of Canada. 1967.

18. Williams, D. E. and Rundle, R. E., J. Am. Chem. Soc., 86, 1660 (1964).

19. Jacobson, R. A., Wunderlich, J. A., and Lipscomb, W. N., Acta Cryst. 14, 589 (1961).

20. Rodgers, J. and Jacobson, R. A. A general Fourier program in PL1 for triclinic, monoclinic, and orthorhombic space groups. U.S. Atomic Energy Commission Report IS-2155 (Iowa State University of Science and Technology, Ames. Institute for Atomic Research). 1969.

21. Busing, W. R., Martin, K. O., and Levy, H. A. A fortran crystallographic least-squares program. U.S. Atomic Energy Commission Report ORNL-TM-305 (Oak Ridge National Laboratory, Tennessee). 1962.

22. Cromer, D. T. and Waber, J. T., Acta Cryst., 18, 104 (1965).

23. Johnson, C. K. A fortran thermal-ellipsoid plot program for crystal structure illustrations. U.S. Atomic Energy Commission Report ORNL-3794 (Oak Ridge National Laboratory, Tennessee). 1965.

24. Dunitz, J. D., Acta Cryst., 2, 1 (1949).

25. "Tables of Interatomic Distances and Configurations in Molecules and Ions", J. Chem. Soc., Special Publication No. 11, 1952 (1958).

26. Busing, W. R., Martin, K. O., and Levy, H. A. A fortran crystallographic function and error program. U.S. Atomic Energy Commission Report ORNL-TM-306. (Oak Ridge National Laboratory, Tennessee). 1964.

27. Burbank, R. D., Inorg. Chem., 9, 1491 (1966).

28. Bauer, D., Schnering, H. G., and Schafer, H., J. Less Common Metals, 8, 388 (1965).

29. Bauer, D. and Schnering, H. G., Z. Anorg. Allgem. Chem., 361, 259 (1968).

30. Simon, V. A., Schnering, H. G., Wohrle, H., and Schafer, H., Z. Anorg. Allgem. Chem., 339, 155 (1965).

31. Simon, V. A. Schnering, H. G., and Schafer, H., Z. Anorg. Allgem. Chem., 361, 235 (1968).

32. Schafer, H., Schnering, H. G., Niehues, K. J., and Nieder-Vahrenholz, H. G., J. Less Common Metals, 9, 95 (1965).

33. Koknat, F. W. and McCarley, R. E., Ames, Iowa. X-ray structural data for $Nb_6Cl_{18}^{4-}$. Private communication. 1969.

34. Wehe, D. J., Busing, W. R., and Levy, H. A. A Fortran program for single crystal orienter absorption corrections. U.S. Atomic Energy Commission Report ORNL-TM-299 (Oak Ridge National Laboratory, Tennessee). 1962.

35. Cromer, D. T., Acta Cryst., 18, 17 (1965).

36. Hackert, M. L., Ames, Iowa. Computer program. Private communication. 1968.

37. Levy, H. A., Acta Cryst., 9, 679 (1956).

38. Cotton, F. A. and Haas, T. E., Inorg. Chem., 3, 10 (1964).

39. Schneider, R. F. and Mackay, R. A., J. Chem. Phys., 42, 843 (1968).

40. Flemeng, P. B. and McCarley, R. E., Inorg. Chem., 00, 000 (1969).

41. Simon, A., Schnering, H. G., and Schafer, H., Z. Anorg. Allgem. Chem., 355, 311 (1967).

42. McCarley, R. E., Ames, Iowa. Chemical evidence. Private communication. 1970.

43. Abowitz, G. and Ladell, J., J. Sci. Instr., 45, 113 (1968).

44. Altona, C., Acta Cryst., 17, 1283 (1964).

45. Read, T. R. and Lipscomb, W. N., Acta Cryst., 6, 45 (1953).

46. Thaxton, C. B. and Jacobson, R. A., J. Phys. E, 3, 245 (1970).

ACKNOWLEDGMENT

The author wishes at this time to express his sincere indebtedness to a few people who have been instrumental in developing in him concepts of eternal value.

To Professor Robert A. Jacobson whose strength of character, sense of fair play, and warm hospitality have served to teach the author by example the concept of biblical grace. His guidance in the author's research is also gratefully acknowledged.

Acknowledgments are in order for Drs. A. Schlueter and P. J. Hansen whose probing and penetrating questions played their part in destroying the author's naive concept of a "southern" god, and putting in its place the grand and glorious one of "the God who is there", as revealed in His Word.

The author also wishes to thank Mr. H. F. Hollenbeck and all the members of the X-ray groups I and II who have contributed greatly in the "graduate student" experience.

And finally the author acknowledges his parents, Mr. and Mrs. Ellis B. Thaxton, who have been continually a source of love, understanding, and encouragement.

APPENDIX. RESEARCH PROPOSITIONS

A literature search has revealed a dearth of accurate solid state structural information regarding compounds containing both silicon and carbon, and concerning cyclobutane rings, planar and non planar. It would be of considerable interest if experimental evidence were available to establish that C-C distances within the cyclobutane ring are significantly longer than the normal C-C single bond length. Since silole dimer contains three different Si-C bond types, and a planar 4-membered ring, it is suggested that a reinvestigation of this material at low temperatures would provide both worthwhile fundamental knowledge and valuable experience in low temperature crystallography. As such it would make a fine "first problem" for a new graduate student.

A literature search should be made of liquid materials, and these arranged according to simplicity and structural importance. A systematic X-ray investigation of single crystals grown <u>in situ</u> from the melt would provide a significant extension to structural knowledge. To the author's mind such a systematic investigation is nowhere being pursued.

Further structural studies of the species $[(M_6X_{12})Y_mL_{6-m}]^{(n-m)+}$ are needed to determine if the Ta_6 polynucleus is more susceptible than the Nb_6 polynucleus to deformation from O_h symmetry. Also needed is more information regarding ligand effect on structure. Of especial interest would be structural data for these cluster compounds in all three oxidation states (n = 2,3,4 +) with fluoride as ligand. One such structural study has been reported (Nb_6F_{15}) which has a Nb-Nb distance significantly shorter than in the metal.